



RESEARCH PAPER



Short divalent ethacrynic amides as pro-inhibitors of glutathione S-transferase isozyme Mu and potent sensitisers of cisplatin-resistant ovarian cancers

Bangtian Xu^{a,b*}, Tingting Tong^{a*}, Xin Wang^{a*}, Fang Liu^{a*}, Xiang Zhang^a, Xiaolei Hu^a, Xinpeng Li^a, Xiaolan Yang^a  and Fei Liao^a 

^aKey Laboratory of Clinical Laboratory Diagnostics of the Education Ministry, College of Laboratory Medicine, Chongqing Medical University, Chongqing, China; ^bDepartment of Pharmacy, University-Town Hospital of Chongqing Medical University, Chongqing, China

ABSTRACT

The linking of ethacrynic acid with ethylenediamine and 1,4-butanediamine gave EDEA and BDEA, respectively, as membrane-permeable divalent pro-inhibitors of glutathione S-transferase (GST). Their divalent glutathione conjugates showed subnanomolar inhibition and divalence-binding to GSTmu (GSTM) (PDB: 5HWL) at $\sim 0.35 \text{ min}^{-1}$. In cisplatin-resistant SK-OV-3, COC1, SGC7901 and A549 cells, GSTM activities probed by 15 nM BDEA or EDEA revealed 5-fold and 1.0-fold increases in cisplatin-resistant SK-OV-3 and COC1 cells, respectively, in comparison with the susceptible parental cells. Being tolerable by HEK293 and LO2 cells, BDEA at 0.2 μM sensitised resistant SK-OV-3 and COC1 cells by ~ 3 - and ~ 5 -folds, respectively, released cytochrome c and increased apoptosis; EDEA at 1.0 μM sensitised resistant SK-OV-3 and A549 cells by ~ 5 - and ~ 7 -fold, respectively. EDEA at 1.7 $\mu\text{g/g}$ sensitised resistant SK-OV-3 cells to cisplatin at 3.3 $\mu\text{g/g}$ in nude mouse xenograft model. BDEA and EDEA are promising leads for probing cellular GSTM and sensitising cisplatin-resistant ovarian cancers.

ARTICLE HISTORY

Received 11 November 2021
Revised 29 January 2022
Accepted 1 February 2022

KEYWORDS



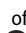

Glutathione S-transferase isozyme mu; divalent pro-inhibitor; slow tight-binding inhibitor; cisplatin-resistance; sensitisation

Introduction


Cytotoxic anticancer agents such as cisplatin (DDP) as single agent or in combination with other agents are widely used for the treatment of solid cancers such as testicular, ovarian, head and neck, bladder, lung, cervical cancers. The pharmacological actions of DDP generally involve its activation into the mono-aquated and di-aquated forms, which in a small part bind to nuclear DNA, and consequently block cell division and result in apoptotic cell death. Moreover, such activated DDP forms in excess also interact with cytoplasmic nucleophiles containing sulfhydryl groups or nitrogen donors, such as mitochondrial DNA (mtDNA) and multiple mitochondrial as well as extramitochondrial proteins, to promote cell fatal lesion and apoptosis through mainly but not limited to (1) the development of oxidative stress; (2) a signal transduction cascade involving the activation of pro-apoptotic BCL-2 family members BAK1 and BAX, as well as mitogen-activated protein kinases represented by both p38MAPK and c-Jun N-terminal kinase 1 (JNK1); (3) the cytoplasmic components of p53 signalling pathway¹. However, resistance of solid cancers to DDP is a great medical challenge². In the cytosol of human cells, glutathione S-transferase (GST; EC 2.5.1.18) has several isozymes that catalyse glutathione (GSH) conjugation with xenobiotics and endogenous compounds³. Inevitably, the actions of GST isozymes may alter the biological actions of those xenobiotics and endogenous compounds as GST substrates. In most solid cancers, GST isozyme pi (GSTP) is abundant, while isozymes alpha (GSTA) and mu (GSTM)

are merely detectable^{4,5}, but the overexpression of GSTP, GSTA, and GSTM has already been found in many solid cancer cells after the development of DDP resistance^{6–9}. To date, GSTP, GSTA and GSTM have been suggested to cause DDP resistance in solid cancers through (1) the catalysed GSH conjugation of DDP itself and/or its secondary mediators to block their actions^{6,8,10}, (2) interactions with cell membrane transporters to promote DDP efflux^{6,10–12} and/or (3) binding as modulators to signalling kinases, such as JNK, ASK1, Akt, or receptors like RyRs and EGFR^{6,8,13–16}. An inhibitor with high affinity and good selectivity for an isozyme of GST is thus a potential sensitiser to DDP in solid cancers whose DDP resistance is caused mainly or partially by the actions of the GST isozyme^{8,10,17,18}. Moreover, a potent and isozyme-selective inhibitor of GST is an important probe to biological and pharmacological roles of the intracellular GST isozyme in biological processes¹⁹. To date, many isozyme-selective inhibitors of GSTs have been reported^{3,6,8,10,20–22}, but are usually unsatisfactory due to their low inhibition potencies, weak selectivity for the isozymes of interest, manifest side effects and/or unfavourable membrane permeability^{6,8,9}.

GST as a dimer has two active sites linked by a narrow cleft¹⁷. In the dimer of GST, each active site has a small G-site for GSH and a large H-site for electrophilic substrates, and the two H-sites of the dimer are directly linked by the cleft. Of GST, a compound that is capable of binding to just one active site is a monovalent ligand, while a compound that is capable of concomitant binding

CONTACT Xiaolan Yang  xiaolangyang666@cqmu.edu.cn, xiaolangyang666@yeah.net  Key Laboratory of Clinical Laboratory Diagnostics of the Education Ministry, College of Laboratory Medicine, Chongqing Medical University, Chongqing 400016, China; Fei Liao  liaoifeish@yeah.net, liaoifeish@cqmu.edu.cn  Key Laboratory of Clinical Laboratory Diagnostics of the Education Ministry, College of Laboratory Medicine, Chongqing Medical University, Chongqing 400016, China

*These authors contributed equally to this work

 Supplemental data for this article can be accessed [here](#).

© 2022 Chongqing Medical University, Chongqing 400016, China.

This is an Open Access article distributed under the terms of the Creative Commons Attribution-NonCommercial License (<http://creativecommons.org/licenses/by-nc/4.0/>), which permits unrestricted non-commercial use, distribution, and reproduction in any medium, provided the original work is properly cited.

to two active sites is denoted a divalent ligand^{17,23–27}. A monovalent electrophilic substrate of GST is a monovalent pro-inhibitor if its GSH conjugate has a higher affinity through the simultaneous binding to both the G-site and H-site of just one active site. To date, few monovalent inhibitors of GST have inhibition constants (K_i) below 0.1 μM and sufficient isozyme selectivity^{10,17,22,28,29}. For example, ethacrynic acid (EAA) and its analogues have been widely investigated as GST inhibitors and sensitizers of tumour cells to the cytotoxic effects of DDP and alkylating agents but exhibit significant side effects at their therapeutic levels^{6,8,9,17,18}. However, divalent inhibitors of GST usually show stronger affinities and better isozyme selectivity through favourable interactions concomitantly with two active sites in the dimer of a GST isozyme, and the additional interactions between the linkers and the cleft^{23–27}. For instance, 2,4-dinitrochlorobenzene (CDNB) and EAA gave GSH conjugates that are monovalent GST inhibitors bearing micromolar K_i values and negligible isozyme selectivity (Supplementary Figure S1)^{17,30}. Fortunately, the linking of two GSH conjugates of an analogue of CDNB *via iso-phthalic acid diacylhydrazine* gave a divalent inhibitor bearing the distance of about 23 atoms between two GS moieties, and thus produced a favourable K_i of ~ 50 nM against GSTM1-1, but a submicromolar K_i against GSTP1-1²⁴. The linking of two EAA molecules *via 3,5-aminomethyl benzamide* (AMAB) in the form of Asp-Gly-AMAB-Gly-Asp yielded a divalent inhibitor with K_i of 42 nM for GSTA1-1²⁵; the linking of two EAA *via AMAB* in the form bearing bis-terminated linear amino acid arms for 1–3 and 5–7 carbon atoms from the benzene ring resulted in divalent inhibitors with K_i of 14–40 nM for GSTA1-1 and 30–50 nM against GSTP1-1, respectively²⁶. Specially, the linking of two EAA molecules *via a trans-Pt IV complex* yielded ethacraplatin with K_i in the submicromolar range against GSTP³¹. The linking of two GSH conjugates of CDNB analogues *via iso-phthalic acid* bearing bis-terminated glycol or propylene glycol arm gave submicromolar K_i for GSTP1-1 and GSTA1-1, and the linking of two bulk unilblue A *via 10-atom linear diamines* gave K_i of ~ 45 nM against GSTP1-1²⁷. However, few reported divalent inhibitors were successfully used as DDP sensitizers in resistant cancer cells *in vitro* and/or *in vivo*^{23–27}, or as research probes of the roles of GST isozymes in cellular activities.

For the inhibitors of GST, the permeation into cells is a general prerequisite for their sensitization actions to DDP in solid cancers and their biological actions inside cells. Reported divalent potent inhibitors^{24–27} usually have negative LogP values due to their conjugation with GSH, large sizes by the use of bulky rigid linkers or bulky H site binding moieties like unilblue A, and/or many H-bonding atoms in the linkers like AMAB and peptides²⁴, and thus insufficient membrane permeability according to Lipinski's rule³². Small monovalent pro-inhibitors of GST usually show good membrane permeability³² and can be converted rapidly to GSH conjugates of higher affinity by the intracellular GST activities and high GSH levels especially in resistant cancer cells (Supplementary Figure S1)^{9,30,33}. Divalent pro-inhibitors derived through the linking of a small monovalent pro-inhibitor *via* suitable linear linkers may have good membrane permeability, and their GSH conjugates as divalent inhibitors *in situ* generated inside cells should exhibit much higher affinities to GSTs^{24–27,30}; thus, they may exert biological actions on common cells and sensitize resistant cancers to DDP. Comparison of the crystal conformations of GSTM (pdb: 3gur), GSTA (pdb: 2vcv) and GSTP (pdb: 1gp) revealed that the distances between two G-sites are about 2.2 nm in GSTM, while about 2.5 nm in GSTA or GSTP; the cleft of GSTM among those three isozymes also shows the weakest steric hindrance for binding of a short linear linker (Supplementary Note S1-Figure S1). Evidently, if

the linear linker of such a divalent inhibitor is short enough, the divalent GSH conjugate may have favourable selectivity for a particular GST isozyme bearing the shortest distance between the two G-sites, and thus GSTM may be the target of such a divalent conjugate. Notably, GSTM was the most predominant isozyme in some DDP-resistant ovarian cancers, and silencing GSTM sensitized these ovarian cancers to DDP^{3,9,13,34}. With EAA as a small monovalent pro-inhibitor whose GSH conjugate has about nine single bonds from sulphur atom to carboxyl carbon of EAA, 1,4-butyldiamine and analogues may be suitable linkers to generate divalent pro-inhibitors against GSTM. Hence, a short divalent pro-inhibitor may act as a sensitizer to DDP in resistant ovarian cancers and become a promising probe to the biological roles of GSTM in cells.

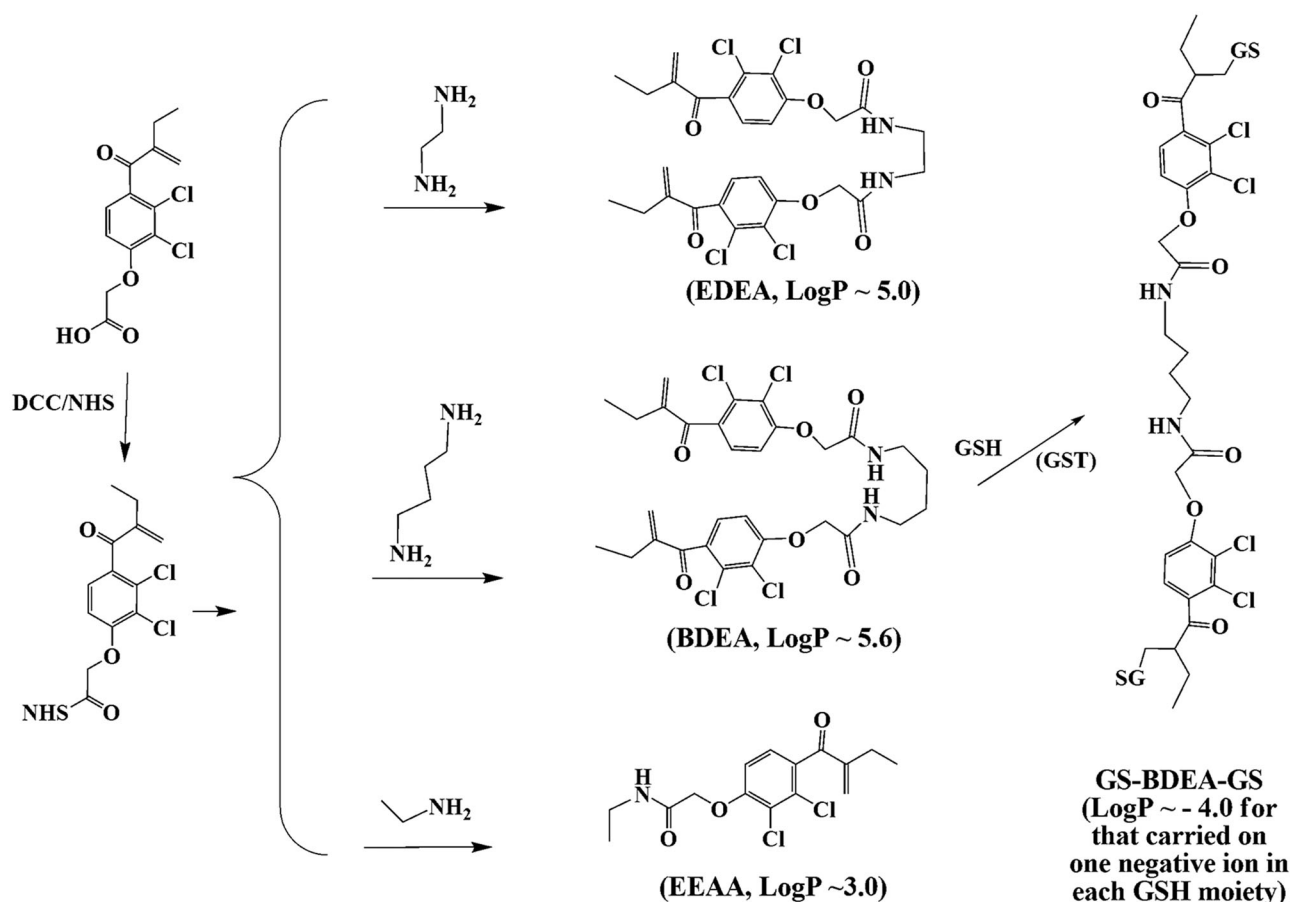
Herein, EAA was linked by ethylenediamine and 1,4-butyldiamine to yield *N,N'*-ethyl-1,4-di-ethacrynic amide (EDEA) and *N,N'*-butyl-1,4-di-ethacrynic amide (BDEA), respectively. Analyses of the biochemical interactions of BDEA and EDEA as well as their divalent GSH conjugates with GSTs, their pharmacological actions on DDP-resistant solid cancers cells *in vitro* and associated action mechanisms, and the pharmacological action of EDEA on xenograft models of representative DDP-resistant solid cancers *in vivo*, supported the design.

Materials and methods

GSH, GSH-Sepharose 4B, ethacrynic acid (EAA), and 2,4-dinitrochlorobenzene (CDNB) are purchased from Sigma-Aldrich (St. Louis, MO). Isopropanyl- β -D-thiogalactoside (IPTG), *Escherichia coli* cell strains, cell counting kit-8 (CCK-8) solution, culture media and poly(vinylidene fluoride) (PVDF) membrane, rabbit anti-human GSTM2 monoclonal antibody, rabbit anti-human GSTA1 monoclonal antibody, rabbit anti-human β -actin monoclonal antibody, and goat anti-rabbit IgG monoclonal antibody labelled with horseradish peroxidase were from Shanghai Sangon Bioengineering Co., Ltd. (Shanghai, China). ImmobilonTM western chemiluminescent substrate kit was from Millipore. SK-OV-3 resistant to DDP (SK-OV-3/DDP hereafter) was from Cell Resource Centre of Shanghai Institute of Biological Sciences, Chinese Academy of Science (Shanghai, China). Ovarian cancer SK-OV-3, human embryonic kidney cell HEK293 and hepatocyte cell LO2 were gifts from Professor Tongchuan He in our laboratory. COC1 and COC1 resistant to DDP (COC1/DDP hereafter) were gifts from Professor Tinghe Yu in our University⁶. RIPA lysis buffer was from Cell Signalling Technology, Inc., <http://www.cellsignal.com/product/productDetail.jsp?productId=9806>. Other chemicals were domestic reagents of analytical grade or better.

Preparation of designed compounds and analyses of structures

EAA was activated for conjugation to diamines (Scheme 1). In detail, EAA (0.50 g, 1.65 mmol) and *N*-hydroxysuccinimide (NHS, 0.20 g, 1.74 mmol) were dissolved in 30 ml tetrahydrofuran (THF), and dicyclohexylcarbodiimide (0.36 g, 1.74 mmol) in THF was added dropwise at 0 °C. After overnight reaction at room temperature, the precipitate was removed, and an amine or diamine was directly added to produce a designed amide compound. As an example, for the preparation of BDEA, 1,4-butyldiamine (0.07 ml, 0.70 mmol) in 10 ml THF was added to the activated ester. After reaction under mild stirring for 6 h, the solvent was removed in vacuum; the residue was dissolved in 20 ml dichloromethane and washed twice, with 50 ml 5% NaHCO₃, 50 ml 0.5 M HCl, and finally a lot of water. After the removal of CH₂Cl₂, the residue was



Scheme 1. Syntheses of the designed pro-inhibitors and the divalent GSH conjugate of BDEA. BDEA: *N,N'*-butyl-1,4-di-ethacrylic amide; EDEA: *N,N'*-ethyl-1,2-di-ethacrylic amide; EEAA: *N*-ethyl ethacrylic amide; GS-BDEA-GS, the divalent product of BDEA

purified through silica gel column by the elution with a mixture of petroleum ether: ethyl acetate: acetic acid at 1:1:0.05. The yield of BDEA or EDEA as white powders was about 0.17 g (~34% with respect to the diamine). To prepare *N*-ethyl ethacrylic amide (EEAA) as a pro-inhibitor, the molar equivalent of ethylamine to EAA was 1.1:1 and the yield was about 50% as white powders. Such compounds had purity > 98% by reverse-phase HPLC (10% water in methanol as the mobile phase under detection of absorbance at 254 nm). Their HNMR and ESI-HRMS data were showed in [Supplementary Note S2-A1](#). Those three pro-inhibitors were dissolved in dimethylformamide (DMF) for calibrating concentrations of the stock solution with EEAA as the reference. The absorptivity of the monovalent pro-inhibitor EEAA detected at 267 nm was $2.57 \text{ (mM)}^{-1} \cdot \text{cm}^{-1}$. Concentrations of EDEA and BDEA were determined by absorbance at 267 nm with the same absorptivity for each EAA moiety.

The divalent product of BDEA was prepared as previously reported³³ with the catalytic action of GSTP. In brief, 100 mg BDEA saturated in 7.0 ml DMF was added to 20 ml solution of $1.4 \mu\text{M}$ GSTP and 16.0 mM GSH for 24 h-reaction at 25 °C. After the removal of GSTP by heating and filtration through 0.22 μm membrane, the residual BDEA by extraction with dichloromethane, and also the solvent through lyophilization, a total of 25 mg white powders was obtained and confirmed by reverse-phase HPLC as well as ESI-HRMS. Concentration of the divalent product of BDEA was determined by absorbance with the monovalent product of EEAA as the reference (Figure 1, [Supplementary Note S2-A2](#) and [A3](#) and [Note S2-Figures S1](#) and [S2](#)).

Expression of GSTs and characterisation of inhibitors

Recombinant expression of human GSTP1-1, GSTM2-2 and GSTA1-1 followed those reported. In brief, pET15b vector bearing GSTP1 (GI: 4504183), GSTM2 (GI: 4504175) or GSTA1 (GI: 22091454) was amplified in *Escherichia coli* DH5 α , and induced for expression in *E. coli* BL21 (DE3) cells by 1.0 mM IPTG for 20 h at 16 °C. Each GST isozyme was purified with GSH-Sepharose 4B column and confirmed for purity by SDS-PAGE ([Supplementary Note S2-A4](#)).

For characterising initial rates of a GST, CDNB and each designed compound were dissolved in dimethylformamide (DMF) to make stock solutions > 5.0 mM. In reaction solutions with GST, final levels of DMF from both CDNB and any candidate inhibitor were kept at no more than 2% to alleviate potential alterations of GST activities. In 100 mM sodium phosphate at pH 6.5, initial rates of GST were measured with CDNB and GSH at 25 °C by recording absorbance at 340 nm at 10-s intervals after a lagging time of 20 s and initial rate was derived from the absorbance change from 30 to 90 s since reaction initiation. Apparent specific activities were calculated from total proteins. To detect the inhibition action of an inhibitor itself, the inhibitor was mixed with CDNB and an isozyme of GST at 25 °C, and GSH was added at last to initiate the reaction and then record the absorbance at 340 nm in 90 s. To detect the inhibition action of a GSH conjugate generated *in situ*, an inhibitor was incubated with GSH in excess and an isozyme for an indicated period at 25 °C, and then CDNB was added at last to initiate the reaction and record the absorbance at 340 nm. For facile comparison of inhibition affinity, half-inhibition concentration (IC_{50}) was estimated with both CDNB and GSH at 1.0 mM.

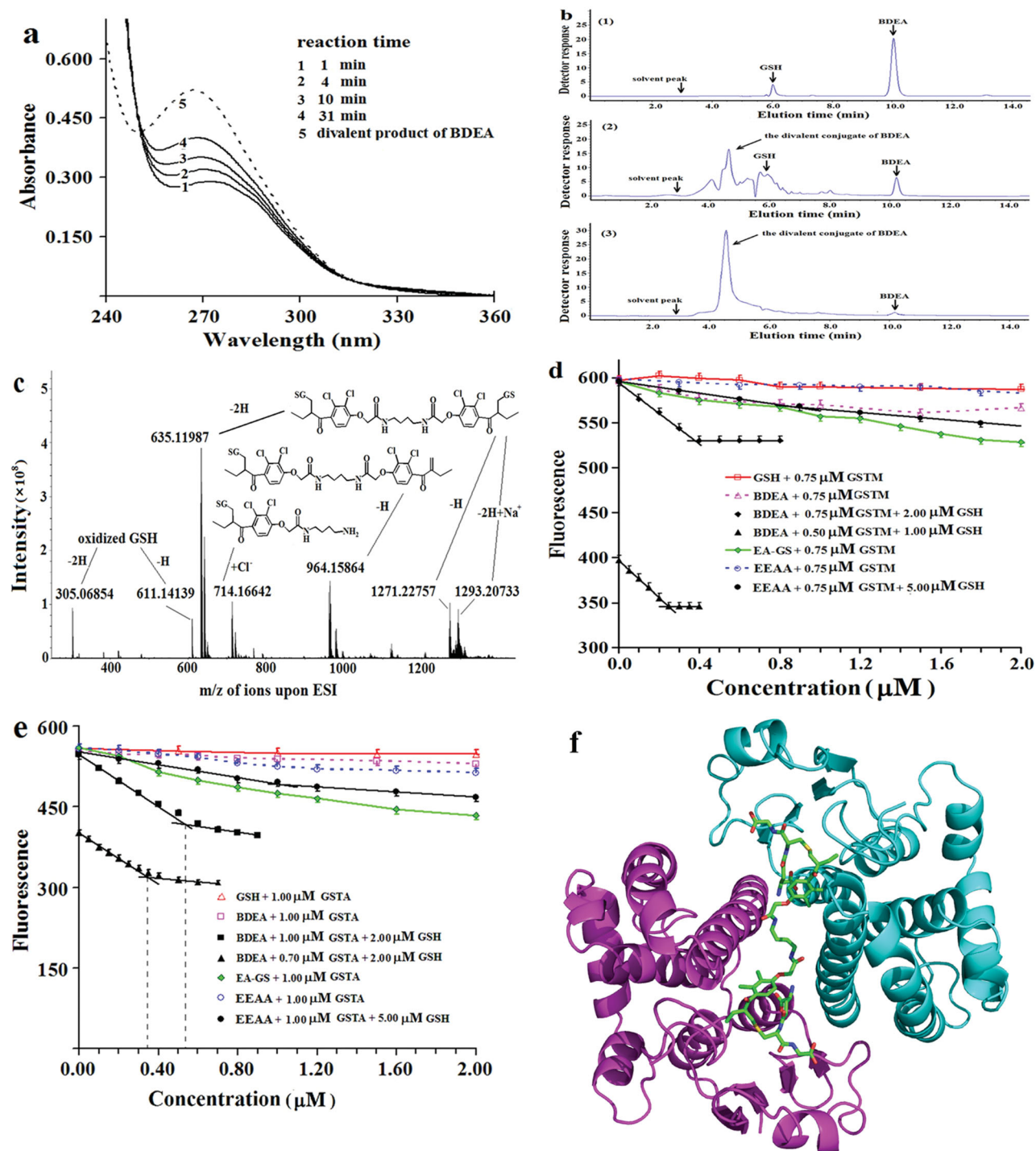


Figure 1. Action properties of pro-inhibitors and the product derived from BDEA. (a) Absorbance change of reaction mixture of GSTA on EEA at 0.10 mM and GSH at 1.0 mM. Lines 1, 2, 3, 4 indicated absorbance spectra after reaction for indicated periods. Line 5 was for the divalent conjugate from BDEA and GSH. (b) HPLC analysis of the conjugates of BDEA and GSH by absorbance at 265 nm. (1) The reaction mixture of BDEA and GSH but no GSTP for 30 min. (2) The reaction mixture of BDEA, GSH and GSTP for 30 min. (3) The reaction mixture of BDEA, GSH and GSTP for 24 h. (c) ESI-HRMS analysis of mixture of GSH, BDEA and GSTP after reaction for 30 min. (d) Fluorometric titration of the active site of GSTM with BDEA plus GSH in excess. EA-GS: GSH conjugate of EAA. (e) Fluorometric titration of the active site of GSTA with BDEA plus GSH in excess. (f) Structure model of the complex of GSTM and the divalent product of BDEA (pdb code: 5HWL). All data as mean \pm SD were repeated trice.

For revealing inhibition types, CDNB was fixed at 1.0 mM for varying GSH levels to estimate Michaelis–Menten constant (K_m) for GSH, while GSH was fixed at 1.0 mM for varying CDNB levels from 0.25 to 1.0 mM to estimate K_m for CDNB. The inhibition type was judged from the response of apparent maximum reaction rates and apparent K_m to inhibitor concentrations³⁵. The K_{iv} was derived from a equation relating V_{m0} in the absence of an inhibitor to the

apparent V_m in the presence of the inhibitor, so as to the K_{ik} , then the larger one among the K_{iv} and K_{ik} was divided by the smaller one to give the ratio, which was used to discriminate the inhibition types according to the rules as we reported previously³⁵.

To approximate K_i for the divalent GSH conjugate of BDEA as a tight binding inhibitor, Eq. (1) considering the binding sites

depletion in GST to develop the equilibrium of the binding reaction between active sites of GST and GSH conjugate was fit to the response curve^{27,36,37}:

$$\frac{v}{v_0} = \frac{(E - I - K_i) + \sqrt{(E - I - k_i)^2 + 4 \times E \times K_i}}{2 \times E} \quad (1)$$

Susceptibility of GST in cell lysates to an inhibitor, and Western-blotting of GSTs

Cells were cultured at 37 °C in flask with RPMI1640 medium containing 10% mycoplasma-free calf serum, gentamycin at 100 mg/l and penicillin G at 100 kU/l under 5% CO₂ atmosphere. After culture for 48 h and digestion with 0.25% trypsin, about 2×10^7 cells were harvested by centrifugation at 13,000 rpm for 10 min. Collected cells were then suspended in 100 μ l RIPA lysis buffer at 4 °C for 30 min and the suspension was mixed at 5.0-min intervals. Finally, the mixtures were centrifuged at 13,000 rpm for 10 min to give supernatants (lysates). To detect the action of the divalent conjugate of BDEA or EDEA on GST activities in cell lysate, each lysate was mixed with GSH in excess and BDEA or EDEA at an indicated level for 10.0 min at 25 °C, and then CDNB was added for final 1.0 mM to record the absorbance change at 340 nm.

For Western-blotting detection of GSTs, 80 μ g proteins from a lysate were loaded for SDS-PAGE. After transferring of separated proteins onto PVDF-membrane, GSTM2, GSTA2 or GSTP1 was detected by monoclonal rabbit antibody recognising the GST isozyme plus goat anti-rabbit IgG polyclonal antibodies labelled with horseradish peroxidase. The reference protein was β -actin. Peroxidase was detected with chemiluminescent substrate kit on Cool-Imager Device (Viagene, Changzhou, China) and quantified with the software Quantity-one.

Inhibition of cell growth and sensitisation of cancer cells to DDP

DDP was dissolved in physiological saline to 5.0 mM and diluted with the culture medium. DMF from inhibitor solutions was limited to below 0.2% in the culture medium. After digestion with 0.25% trypsin, cells during exponential growth were harvested and then diluted with culture medium to 5×10^7 /l. Aliquots of cell suspension of 20 μ l were applied to microplate wells for determining IC₅₀ of DDP. After culture of such cells for 24 h at 37 °C and the addition of an inhibitor when indicated, DDP for an indicated final level was added in an hour. After further culture of cells for 72 h at 37 °C, CCK-8 solution of 10 μ l was added for 2-h reaction before the assay of absorbance at 450 nm with Biotek ELX 800 microplate reader (BioTek, Winooski, VT). The percentage of live cells was the ratio of absorbance of a test to that minus DDP and the inhibitor. Data were determined in triplicate. Low toxicity indicated < 10% inhibition of cell growth.

Sensitisation action of EDEA to DDP on xenograft models of DDP-resistant cancers

BALB/c nude mice (6-week age, mean body weight 20 g) were purchased from Shanghai National Centre for Laboratory Animals and kept in a specific pathogen-free environment where the temperature was maintained at 22 °C and humidity kept in the range of 40–50%. All animal experiments were approved by the Animal Ethics Committee of Chongqing Medical University, and all the procedures were in accordance with the National Institutes of Health Guidelines for Animal Research of China (Guides for Care and Use of Laboratory Animals). EDEA was suspended in 0.2% tween 80 and 0.1% dimethylsulphoxide (DMSO). In 0.10 ml cell

suspension, 1×10^7 cells of SK-OV-3/DDP, A549/DDP or SGC7901/DDP were injected *via* inguinal lateral to BALB/c nude mice; DDP at 3.0 mg/kg was introduced every 3 days for six times in total to develop a xenograft model of DDP-resistant solid tumour³⁸. Three weeks after transplantation of cancer cells, solid tissues of cancers reached 5–10 mm in diameter. Afterwards, tumour-loaded Balb-c nude mice were divided into four groups for treatment once a week with DDP alone at 3.0 μ g/g, EDEA alone at 1.7 μ g/g body weight³⁹, EDEA at 1.7 μ g/g plus DDP at 3.0 μ g/g, or physiological saline plus 0.2% tween 80 and 0.1% dimethylsulphoxide. Tumour volume (V , mm³) was calculated as $V = 1/2 \times a \times b^2$, which together with body mass of mice was measured every 2 days. The treatment lasted for 18 days before mice were sacrificed for characterisation. Images were taken with CANON DIGITAL 1XUS860IS.

Binding kinetics of the divalent product derived from BDEA and GSH to GSTM

The mixture in 1.2 ml contained CDNB at final 1.0 mM, GSTM at final 2.5 nM, and 25 nM of the divalent product derived from BDEA and GSH, and was allowed to react for an indicated time. GSH was then added for final 1.0 mM to initiate the enzyme reaction. After a lag-time of 12 s, the absorption at 340 nm was recorded every 10 s in 90 s since the addition of GSH. The residual activities were plotted against the time of binding reaction for revealing the kinetics.

Crystallisation of the complex of GSTM and resolution of its structure model

GSTM was purified through affinity chromatography twice. To prepare the complex for crystallisation, a total of 26 mg GSTM (~1.0 micromole of subunit) was dissolved in 5.0 mM Tris-HCl at pH 7.5 to 100 ml containing final 0.024 mM GSH; BDEA of 0.40 mg in 0.30 ml DMSO (for the final level < 0.5% in reaction mixture) was added dropwise into the mixture for reaction of 60 min at room temperature. The resulted reaction mixture as the binding sample was concentrated *via* ultra-filtration to ~0.60 ml. Using the sitting drop vapour diffusion method for preliminary screening, 1.0 μ l of binding sample with 1- μ l/well of Hampton kit (including Index, Salt1, Salt2, PEGRx1, PEGRx2, PEG Screen I, PEG Screen II) were mixed for growing of the crystal at 20 °C. Index 59 was then selected for further optimisation using suspended drop gas phase diffusion method until the single crystal with strong diffraction capacity was obtained. For final crystallisation by vapour phase diffusion in sitting drop mode, the final condition used 0.10 M HEPES at pH 6.8 plus 0.02 M MgCl₂, 30% (w/v) poly-(acrylic acid sodium salt)-5100, the complex of GSTM and its divalent inhibitor at ~0.40 g/l. The cryoprotectant solution contained 20% (v/v) ethylene glycol, 0.02 M magnesium chloride hexahydrate, 0.10 M HEPES pH 6.8 and 30%w/v poly (acrylic acid sodium salt) 5100.

Diffraction data were collected at beamline BL17U of Shanghai Synchrotron Radiation Facility (SSRF, Shanghai, China) at 100 K and a wavelength of 0.97915 Å. The data were indexed and scaled by IMOSFLM and SCALA as implemented in CCP4 (Collaborative Computational Project, number 4), respectively⁴⁰. The crystals belonged to the space group P1211 and diffracted to 1.6 Å. Using PDB accession code 1XW5 of human GSTM as the search model, initial phases were determined by molecular replacement with as-implemented program in CCP4 suite⁴¹. Cycles of manual adjustment using Coot and subsequent refinement using PHENIX led to a final model with a R factor (R_{cryst}) of 17.92% and a free R factor (R_{free}) of 20.55% at 1.60 Å resolution^{42,43}. Crystal property data

were collected in [Supplementary Note S1-Table S1](#), and the structure model was deposited in PDB with the accession code of 5HWL.

Results

Design of divalent pro-inhibitors selective for GSTM

In the active site of GST, the G-site usually has a stronger affinity for the GSH moiety than the H-site for their common electrophilic substrates, supporting the design of a divalent pro-inhibitor that yields a divalent GSH conjugate with two GSH moieties for concomitant binding to the G-sites of the two active sites in a GST dimer. With a divalent GSH conjugate bearing a long enough linear linker, two GSH moieties can be easily bound in the G-sites of two active sites of a GST dimer *via* the interaction mode of GSH in the respective monovalent conjugate regardless of the binding of the linear linker^{24–27}. Inevitably, such a long divalent GSH conjugate has weak isozyme selectivity. For good isozyme selectivity of a divalent GSH conjugate, the cleft between the two active sites in GST can be an additional domain to bind the linear linker. If the linear linker is short enough, two GSH moieties in the divalent conjugate can bind to two G-sites of a dimer *via* the mode of GSH in a monovalent conjugate only when the linear linker is bound completely within the cleft. Such a short divalent GSH conjugate should be specific for a GST isozyme whose cleft has negligible hindrance for the binding of the linker and whose distance between two G-sites is the shortest. A linker with suitable length, flexibility and chemical properties, to enable the concomitant favourable bindings of two GS moieties to the two G-sites, two electrophilic moieties to two H-sites in GST dimer and the linker to the cleft, are desired for the design of the divalent pro-inhibitor with high isozyme selectivity.

Among the three common isozymes mentioned above, GSTM had both the cleft bearing negligible steric hindrance for the binding of a linear linker and the shortest distance between the G-sites of the two active sites ([Supplementary Note S1-Figure S1](#)). Comparison of the conformations of the docked complexes of the divalent GSH conjugate of BDEA with the three GST isozymes supported that the use of linear diamines bearing just 4–6 atoms as the linkers can give divalent GSH conjugates that exhibit reasonable selectivity for GSTM. As a research tool, an inhibitor of GST is preferred to have both affinity and isozyme selectivity that are as high as possible. Different profiles of GST isozymes are associated with DDP resistance in different solid cancers^{2,4,5,7–9,34}. The strong affinity of an inhibitor to GST isozymes, rather than the selectivity for just one isozyme, provides greater promise for the inhibitor to be a universal sensitiser to DDP in common cancer cells. DDP resistance in SK-OV-3 ovarian cancer cells requires the actions of GSTM^{4,5,7}. GSTM-selective membrane-permeable divalent pro-inhibitors may thus be sensitisers of SK-OV-3/DDP and probes of GSTM roles in cellular activities.

EAA, as a monovalent pro-inhibitor, has favourable membrane permeability according to Lipinski's rule³² and corneum/water partition coefficient⁴⁴, the free carboxyl group for reaction, and known toxicological properties at therapeutic levels⁹. EDEA and BDEA were thus prepared from EAA with ethylenediamine and 1,4-butyl-diamine as the linear linker, respectively. Comparison with EAA and *N*-ethyl ethacrynic amide (EEAA) as the parental monovalent pro-inhibitors, BDEA and EDEA were characterised for their interactions with GSTM, GSTA and GSTP (Note S2-A4) and sensitisation actions to DDP in SK-OV-3/DDP, COC1/DDP, SGC7901/DDP and A549/DDP cells as DDP-resistant solid cancers.

Biochemical interactions of EDEA and BDEA with three GST isozymes

The production of GSH conjugates of EDEA, BDEA and EEAA under the catalytic action of GST plus GSH was examined. (a) There was a continuous increase in absorbance at 265 nm during incubation of any of the three GST isozymes with 1.0 mM GSH and 0.10 mM EEAA ([Figure 1\(a\)](#)). (b) In the mixture after incubation of GSTP, GSH (in excess) and BDEA for 24 h at 25 °C to exhaust BDEA, just one new entity of higher mobility was detected on reverse-phase HPLC by absorbance at 265 nm ([Figure 1\(b\)](#) and [Supplementary Note S2-A3](#)). (c) In the mixture after incubation of GSTP with BDEA and GSH at comparable levels for 30 min, both the divalent and monovalent conjugates of BDEA with GSH were detected by ESI-HRMS ([Figure 1\(c\)](#)). Therefore, BDEA, EDEA and EEAA are substrates of the tested GST isozymes to give their GSH conjugates.

The inhibition potencies and isozyme selectivity of the designed compounds and their GSH conjugates were compared. When GSH was added at last to initiate the reaction with CDNB, there was negligible formation of the GSH conjugate of the designed compound during the assay of the initial rate of GST over a short period. In this case, the analysis of the response of initial rates of GST to the concentrations of the designed compound gives an approximation of the apparent IC₅₀ of the designed compound itself, even if it is a pro-inhibitor. In contrast, after a long enough period of preincubation of GST and a designed pro-inhibitor with an excess of GSH, the apparent IC₅₀ should reflect the affinity of the GSH conjugate generated *in situ*, and the reduction of such apparent IC₅₀ values *versus* that without preincubation supports that it is a pro-inhibitor.

When GSH was added at last to measure GST activity over a short period, the apparent IC₅₀ of BDEA itself against GSTM was ~ 0.1 μM, showing selectivity for GSTM at ~ 47-fold over GSTP and at ~ 12-fold over GSTA, in addition to an affinity for GSTM at ~ 100-fold over that of EEAA or EAA as a monovalent pro-inhibitor on any one of those three isozymes ([Supplementary Table S1](#)). Moreover, the affinity of EDEA itself for GSTM versus those for both GSTP and GSTA was ~15-fold greater. As expected, EEAA and EAA as well as their GSH conjugates showed no selectivity among those three isozymes ([Supplementary Table S1](#)). Interestingly, when EDEA or BDEA was preincubated with one of those three isozymes plus an excess of GSH for 10.0 min to completely convert EDEA or BDEA into the GSH conjugate before the addition of CDNB to measure the initial rates over a short period, the apparent IC₅₀ on GSTM was reduced to (0.008 ± 0.003) μM (*n* = 5) for BDEA and (0.009 ± 0.003) μM (*n* = 5) for EDEA, showing the selectivity for GSTM to be ~ 93-fold over GSTP and ~ 62-fold over GSTA; in addition, the affinity of the conjugate of BDEA or EDEA for GSTM was at >100-fold over that of the GSH conjugate of EEAA or EAA ([Supplementary Table S1](#)). Clearly, the selectivity for GSTM over GSTP of the divalent conjugate of EDEA or BDEA was much stronger than that of the pro-inhibitor and was comparable to that of the divalent inhibitor derived through linking two bulky anthroquinone rings *via* a long linear diamine²⁴. Notably, the IC₅₀ of the divalent GSH conjugate of EDEA or BDEA on GSTM was smaller than those for almost all of the divalent inhibitors reported to date^{24–27}. Hence, BDEA and EDEA are potent pro-inhibitors of GSTM among the tested isozymes.

The binding ratios of these divalent GSH conjugates to the active sites of the GST dimers were approximated ([Supplementary Note S2-A5](#)). When the concentration of BDEA was comparable to that of the active sites of an isozyme of GST, there can be complete conversion of BDEA into its conjugate in a short time in the presence of excess GSH. GSTM and GSTA have tryptophan

residues near their active sites. The fluorescence of the tryptophan residues in GST at 340 nm under excitation at 280 nm was susceptible to the binding of ligands. Binding ratios of the divalent conjugate from BDEA plus excess GSH to GSTM and GSTA were thus estimated *via* fluorometric titration³⁶. GSH, BDEA and their conjugate had negligible fluorescence signals at 340 nm under excitation at 280 nm. GSH or BDEA alone slightly quenched the fluorescence of GSTM and GSTA at 340 nm. At final levels > 0.10 μ M of GSTM or GSTA plus excess GSH, the fluorescence of the reaction mixtures at 340 nm became steady 40 s after the addition of BDEA, supporting the rapid conversion of BDEA into its GSH conjugate under the tested conditions. After preincubation for 5.0 min with an isozyme at a concentration of no more than 1.0 μ M and GSH at levels of no less than the concentration of the EAA moiety, the binding of the conjugate of GSH and BDEA greatly quenched the fluorescence of both GSTA and GSTM. When the concentrations of the conjugate of GSH and BDEA were much lower or higher than that of the concentration of the GSTM active sites, there was a linear response between the fluorescence and the concentration of BDEA; the extensions of the two linear response curves at much lower and higher concentrations of BDEA in the presence of excess GSH thus gave an intersection point as the approximation of the molar binding ratio²⁵. Accordingly, the conjugate of BDEA in the presence of excess GSH had a molar binding ratio of 0.45 ± 0.03 ($n = 3$) to the active sites of GSTM (Figure 1(d)). However, the EAA conjugate had a binding ratio of 0.93 ± 0.04 ($n = 3$) to the active sites of GSTM (Figure 1(d)). Similar binding ratios but smaller slopes indicating less potencies of the divalent conjugate for GSTA were observed (Figure 1(e); Supplementary Table S1). Hence, BDEA and EDEA were the designed divalent pro-inhibitors of tested GST isozymes.

To verify the binding mode of the divalent conjugate of GSH and BDEA to GSTM, the crystal structure of their complex was determined at 1.60 Å resolution (code: 5HWL; Supplementary Note S1-Table S1). The divalent conjugate indeed bound to GSTM as designed (Figure 1(f)). In detail, the short linear diamine linker was entirely bound in the cleft; two GSH moieties were accommodated in the G-sites of the two active sites, while two EAA moieties were located in the two H-sites. Notably, the binding mode of the GSH moieties in the divalent conjugate was similar to that in the monovalent conjugate. Therefore, the divalent GSH conjugate of BDEA had the designed divalent binding mode.

To study direct interactions with GSTM, the divalent GSH conjugate of BDEA was generated enzymatically and purified. GSTP was most effective for GSH conjugation to EEA and the divalent conjugate showed the least inhibition on GSTP among the tested isozymes (Supplementary Table S1), and was thus utilised as the tool for the enzymatic preparation of the divalent GSH conjugate of BDEA. The divalent conjugate has very low solubility in organic solvents and no effective binding on reverse-phase column for chromatographic purification to challenge the purification process, and was thus prepared with one molar quantity of BDEA plus two molar quantities of GSH under the catalytic action of GSTP (Supplementary Note S2-A2). Residual BDEA was removed via extraction with dichloromethane. HPLC analysis revealed less than 2% of the mono-conjugate of BDEA in the preparation (Figure 1(b) and Supplementary Note S2-A2).

Of the divalent conjugate of BDEA and GSH, the binding processes to GSTM, GSTP and GSTA were compared. Of the divalent conjugate, the binding process to GSTM was firstly characterised by changes in the apparent IC_{50} versus the pre-incubation periods with GSTM alone. Of the purified divalent conjugate of BDEA with 4.0 nM GSTM, the apparent IC_{50} was ~ 9.5 nM without pre-

incubation, but ~ 7.5 nM and ~ 5.5 nM after pre-incubation for 2.0 and 5.0 min, respectively, and showed no further changes after pre-incubation for no less than 10.0 min (Supplementary Table S2). The decreases in the apparent IC_{50} values versus the pre-incubation periods indicated slow binding of the divalent conjugate to GSTM³⁷. Such effects of pre-incubation periods on the apparent IC_{50} values of the divalent conjugate were negligible with GSTA and GSTP (Figure 2(a) and Supplementary Table S2). The divalent conjugate was thus a conventional inhibitor of GSTA and GSTP, with weaker affinity, as supported by the apparent IC_{50} values. However, after pre-incubation of the divalent conjugate with GSTM and 1.0 mM GSH for 3.0–10.0 min, the apparent IC_{50} became increasingly larger (Figure 2(a)), supporting competitive binding of the divalent conjugate against GSH for the G-sites of the active sites. For the monovalent conjugate of EAA and GSH, the presence and absence of GSH after a pre-incubation time of 10.0 min gave consistent apparent IC_{50} values on GSTM, and the apparent IC_{50} values of the monovalent conjugate were much larger than that of the divalent conjugate on GSTM. The divalent GSH conjugate of BDEA was thus a slow binding inhibitor to GSTM.

The inhibition constant (K_i) of the divalent conjugate of BDEA to GSTM was estimated. After pre-incubation of the purified divalent conjugate with GSTM alone for 10–30 min to achieve divalent binding, the analysis of the responses of residual activities of GSTM to the total concentrations of the divalent conjugate, according to a model for a slow tight-binding inhibitor (Methods Equation (1))^{27,36}, gave an apparent K_i of (0.48 ± 0.04) nM ($n = 3$). The divalent conjugate of BDEA and GSH was thus a slow tight-binding inhibitor to GSTM with the highest affinity in searchable data^{8,10,17,22,24–27,29,31}.

The rate constant for the divalent conjugate of BDEA to achieve divalent binding to GSTM was approximated. According to the conformation of the divalent conjugate of BDEA with GSTM in the complex, the movement of the linker into the bottom of the cleft is required for the conversion of the divalent conjugate from monovalent binding to divalent binding or the binding of one leftover GSH moiety to the nearby active site for divalent binding (Supplementary Note S1-Figure S2). Namely, binding of the linear linker into the cleft should be the rate-limiting step for divalent binding of the divalent conjugate of BDEA. The strong affinity of the divalent conjugate for GSTM indicates so slow a rate for the dissociation of the complex from the divalent binding state that the complex in the divalent binding state should appear inactive when the residual activity is determined by the absorbance change over a short period after the synchronous addition of GSH and CDNB. When the divalent conjugate is in a large excess to the active sites of GSTM, the complexes with one and two of divalent conjugates in monovalent binding states are still active but slowly converted to the inactive divalent binding state. Accordingly, the residual activities of GSTM may follow a single-component first-order decrease *versus* the binding periods until all of the GSTM molecule is bound by the divalent conjugate in the inactive divalent binding state (Figure 2(b) and Supplementary Note S1-Figure S2). Due to competitive binding against GSH, there was negligible inhibition of GSTM at 2.5 nM from the purified BDEA divalent conjugate at 20 nM after reaction for 3.0 min in the presence of both GSH and CDNB at final concentrations of 1.0 mM. As a result, the binding process of the divalent conjugate was reflected as residual activities of GSTM in 90 s after rapid mixing of an aliquot of the binding reaction mixture with the pre-mixed solution of GSH and CDNB for their final concentrations of 1.0 mM and final concentrations of the divalent conjugate < 20 nM. The rate constant for converting the divalent conjugate of

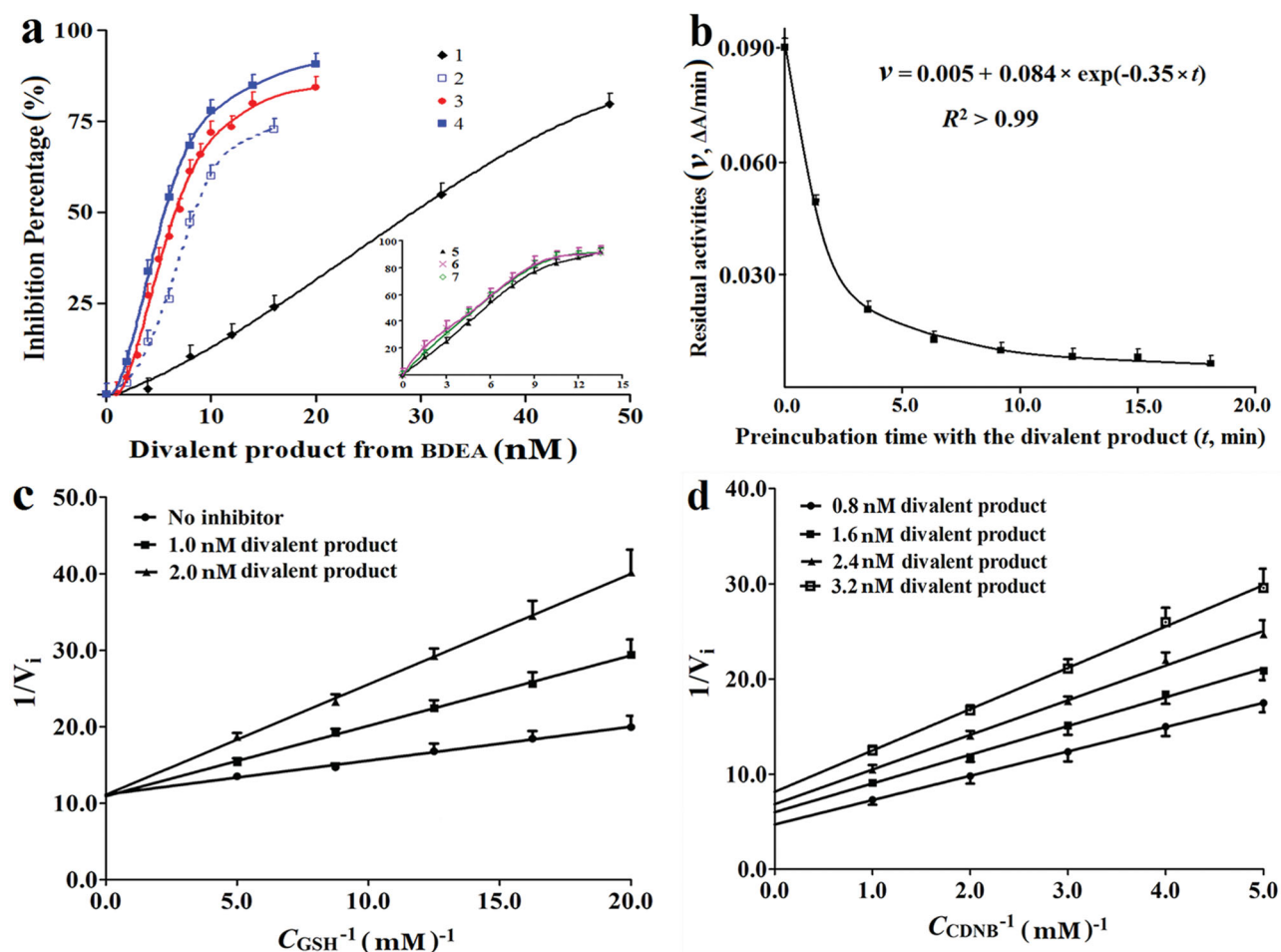


Figure 2. Binding kinetics to GSTM of BDEA and its divalent conjugate. (a) Effects of pre-incubation periods on the inhibition potency on GSTM of the purified divalent conjugate of BDEA. 1 for no pre-incubation; 3 for pre-incubation of 5.0 min with GSTM at 4.0 nM plus 1.0 mM GSH; 2, 4, 5, 6 and 7 indicated pre-incubation for 3.0, 5.0, 10, 20, and 30 min, with GSTM alone at 4.0 nM (without GSH), respectively. (b) Decrease of GSTM activities during reaction with the purified divalent conjugate from BDEA. Final GSTM was 20 nM while the final concentration of the purified divalent conjugate was 100 nM. An aliquot of the reaction mixture was withdrawn at an indicated time and rapidly mixed with an 8-fold volume of a solution of GSH and CDNB for final 1.0 mM to prevent the further formation of the divalence-binding complex and measure the residual activity of GSTM in 2.0 min. (c) Inhibition type of the divalent conjugate from BDEA on GSTM against GSH. From the changes of apparent maximum rates and apparent Michaelis–Menten constants, K_{iv} and K_{ik} were estimated and the ratio of the larger one of K_{iv} and K_{ik} to the smaller one was derived to discriminate the inhibition types³⁵. (d) Inhibition type of the divalent conjugate of BDEA on GSTM against CDNB³⁵. All data were repeated thrice, and expressed as mean \pm SD.

BDEA from monovalent binding to divalent binding was thus $\sim 0.35 \text{ min}^{-1}$ (Figure 2(b)). GSTM had an activity of $\sim 300 \text{ kU/g}$ at 25°C with GSH and CDNB at 1.0 mM (Table 1), indicating a catalytic conversion rate constant of $\sim 8000 \text{ min}^{-1}$. The divalent binding of the divalent conjugate of BDEA to GSTM was achieved at a rate too much slower than that for its catalytic conjugation rate with GSH.

The inhibition types of BDEA and its divalent conjugate were compared. K_{iv} was derived from the response of the apparent V_m to inhibitor concentrations, while K_{ik} was derived from the response of the apparent K_m to inhibitor concentrations³⁵. The ratio of the larger one of K_{iv} and K_{ik} to the smaller one was used for comparison with a preset threshold to judge the inhibition types. After preincubation with GSTM alone for 10.0 min to achieve divalent binding, the divalent conjugate appeared as a competitive inhibitor against GSH (Figure 2(c)), but a non-competitive inhibitor against CDNB (Figure 2(d)). Such inhibition types were similar to other divalent inhibitors^{31–34}, and consistent with the binding mode of the divalent conjugate. BDEA itself was a non-competitive inhibitor against CDNB and a mixed inhibitor

against GSH (Supplementary Figures S2 and S3). The action properties of a pro-inhibitor and the large H-site of GST should account primarily for these inhibition types of BDEA and its divalent GSH conjugate.

Rationale for GSTM as a sensitisation target of representative DDP-resistant cancer cells

The pharmacological actions of DDP on cancer cells involve both DDP itself and intracellular chemical entities as the secondary mediators¹, and the reduction of the intracellular levels of DDP itself and/or its secondary mediators in solid cancers is thus a straight-forward mechanism of DDP-resistance involving GST actions. If the catalytic activities of GSTM for GSH conjugation of DDP and/or those intracellular secondary mediators reduce their intracellular levels to cause DDP resistance, GSTM can be a sensitisation target of DDP-resistant cancers. To date, these intracellular chemical entities have not been fully elucidated², preventing an assay of the catalytic activities of GSTs on their GSH conjugations. In most cancer cells, the development of DDP resistance is

Table 1. Sensitisation of the tested cells to DDP by EDEA and BDEA.

Cell strains	IC ₁₀ of EDEA alone (μM)	IC ₅₀ of EDEA alone (μM)	IC ₅₀ of DDP in the presence of EDEA	
			EDEA (μM)	IC ₅₀ of DDP (μM)
HEK293	1.2 ± 0.5	3.2 ± 0.6	0	2.6 ± 0.5
			0.5	3.2 ± 1.0
			1.0	2.5 ± 1.0
LO2	1.1 ± 0.4	4.0 ± 0.8	0	4.2 ± 0.4
			0.5	4.5 ± 0.5
			1.0	2.7 ± 0.6*
A549	0.7 ± 0.1	1.1 ± 0.1	0	2.5 ± 0.2
			0.5	2.7 ± 0.2
			1.0	<0.3*
A549/DDP	0.5 ± 0.1	1.6 ± 0.1	0	17.6 ± 1.7
			0.5	9.2 ± 1.5*
			1.0	< 2.5
SGC7901	1.5 ± 0.4	4.2 ± 0.2	0	2.5 ± 0.6
			1.0	2.8 ± 0.5
			1.5	<0.1
SGC7901/DDP	1.8 ± 0.6	4.5 ± 1.1	0	8.1 ± 1.2
			1.0	5.5 ± 0.1*
			1.5	1.7 ± 0.8*
SK-OV-3	1.6 ± 0.3	2.5 ± 0.6	0	<0.5
			1.0	4.6 ± 0.8
			1.5	5.9 ± 0.2
SK-OV-3/DDP	3.5 ± 0.4	6.6 ± 0.8	0	2.6 ± 0.7*
			0.5	17.8 ± 0.5
			1.0	15.7 ± 1.1
COC1	0.4 ± 0.1	1.0 ± 0.1	0	3.5 ± 0.8*
			1.0	4.8 ± 0.2
			1.0	2.2 ± 0.3*
COC1/DDP	0.8 ± 0.1	1.3 ± 0.3	0	18.1 ± 1.3
			1.0	7.7 ± 0.2*
			1.0	
Cell strains	IC ₁₀ of BDEA alone (μM)	IC ₅₀ of BDEA alone (μM)	IC ₅₀ of DDP in the presence of BDEA	
			BDEA (μM)	IC ₅₀ of DDP (μM)
HEK293	0.2 ± 0.1	0.7 ± 0.1	0	4.1 ± 0.1
			0.1	4.0 ± 0.1
			0.2	8.4 ± 0.2
LO2	0.2 ± 0.1	2.5 ± 0.2	0	8.3 ± 0.2
			0	1.1 ± 0.1
			0.2	1.1 ± 0.1
SK-OV-3	0.9 ± 0.1	4.9 ± 0.4	0	9.0 ± 0.2
			0.2	6.8 ± 0.2*
			0.035	2.3 ± 0.2*
SK-OV-3/DDP	4.8 ± 0.8	ND	0	2.0 ± 0.2*
			0.2	1.3 ± 0.1*
			0.5	2.2 ± 0.2
COC1	0.2 ± 0.1	2.1 ± 0.5	0	1.9 ± 0.2
			0.2	16.7 ± 0.9
			0	6.3 ± 0.6*
COC1/DDP	0.2 ± 0.1	1.8 ± 0.3	0	5.1 ± 0.4*
			0.035	3.2 ± 0.3*
			0.08	
			0.2	

Each assay with data in triplicate to get the mean ± SD for the estimation of IC₁₀ and IC₅₀. Low toxicity indicated 10% inhibition of cell growth. ND: no detection. **p* < 0.05 versus that without inhibitors by *t*-test.

associated with the changes in the protein levels of multiple GST isozymes^{4,5,7-9}, but GSTM among the tested isozymes showed the highest catalytic activity on CDNB (Supplementary Table S1). For cancers, the increases in the total GST activity on CDNB in cell lysates after the development of DDP resistance implies the potential dependence of DDP resistance on the catalytic activity of GSTM. Moreover, since the divalent conjugate of BDEA or EDEA was a slow tight-binding inhibitor to GSTM with the *K_i* at ~0.48 nM but a conventional inhibitor to other tested isozymes with the IC₅₀ values in the submicromolar range (Supplementary Table S2), the catalytic activity of GSTM on CDNB in cell lysate can be approximated as the GST activity susceptible to the inhibition of a designed divalent GSH conjugate at levels less than 20% of its smallest IC₅₀ value on isozymes other than GSTM but higher than 5-fold of the *K_i* on GSTM. In comparison to DDP-susceptible

parental cancer cells, the increases in GSTM activity on CDNB or total GST activity in cell lysates of DDP-resistant cancer cells thus provide the opportunity for the sensitisation to DDP by BDEA or EDEA at reasonably high levels, while the concomitant increase in GSTM activity and total GST activity in cell lysates imply potential sensitisation to DDP by BDEA or EDEA even at relatively low levels.

In LO2 and HEK293 cell lysates, the total GST activities in soluble proteins were 0.23 ± 0.03 kU/g and 0.17 ± 0.02 kU/g, respectively. In COC1 and COC1/DDP cell lysates, the total GST activities in soluble proteins were 0.36 ± 0.03 kU/g and 0.75 ± 0.08 kU/g, respectively, supporting the induction of GSTs after the development of DDP resistance in COC1 cells. In lysates of SK-OV-3/DDP versus SK-OV-3 cells, a stronger increase in total GST activity was observed. However, the activity of total GSTs showed a negligible difference in lysates of SGC7901/DDP versus SGC7901 cells or in

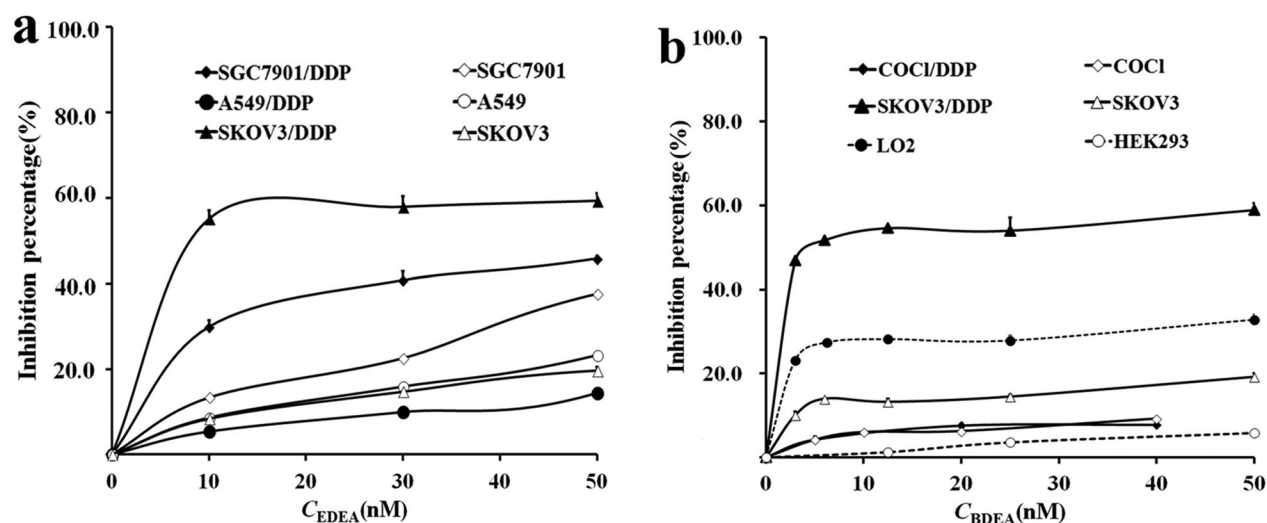


Figure 3. Percents of GST activities in cell lysates susceptible to (a) EDEA and (b) BDEA. (a) The response of residual GST activities to final EDEA concentrations. (b) The response of residual GST activities to final BDEA concentrations. BDEA or EDEA was pre-incubated with GSH in excess plus a cell lysate for 10 min before the addition of CDNB to measure the activity. All data were repeated thrice, and expressed as mean \pm SD.

lysates of A549/DDP versus A549 cells⁷, and were comparable to those in the lysates of LO2 and HEK293 cells. The tested ovarian cancer cells may thus be reasonably susceptible to the sensitisation actions of BDEA or EDEA.

In cell lysates containing EDEA or BDEA plus excess GSH after pre-incubation for 10 min to effectively convert the designed pro-inhibitor into its divalent conjugate, the percent of the inhibited GST activity to total GST activity showed a sharp increase at inhibitor concentrations $<$ 15 nM, a plateau at inhibitor concentrations from 15 to 50 nM, and a slow but progressive increase at inhibitor concentrations $>$ 50 nM until a plateau was again reached at inhibitor concentrations $>$ 200 nM (Figure 3 and Supplementary Figure S4). To approximate the GSTM activity in cell lysates, the level of BDEA or EDEA was thus preset at 15 nM for selective inhibition of GSTM.

The percentage of GSTM activity to total GST activity probed by BDEA or EDEA at 15 nM was \sim 60% for SK-OV-3/DDP versus \sim 8% for SK-OV-3 cells, \sim 29% for SGC7901/DDP versus \sim 13% for SGC7901 cells, \sim 10% for both A549/DDP and A549 cells, and \sim 8% for both COC1 and COC1/DDP cells (Figure 3). Accordingly, BDEA or EDEA at relatively low levels may sensitise only SK-OV-3/DDP cells. However, the percent of GST activity inhibited by BDEA or EDEA at 200 nM to total GST activity reached \sim 35% and \sim 75% in SK-OV-3 and SK-OV-3/DDP cells, and \sim 25% and \sim 45% in COC1 and COC1/DDP cells, respectively, while they reached \sim 80% in both SGC7901/DDP and SGC7901 cells and \sim 70% in both A549/DDP and A549 cells (Supplementary Figure S4), supporting the potential sensitisation of SGC7901/DDP cells and A549/DDP cells by EDEA or BDEA at high concentrations. Western blotting supported the induction of GSTA in all of the tested DDP-resistant cancer cells versus their respective susceptible cells⁷ (Supplementary Figure S5), while GSTP was induced in SK-OV-3/DDP versus SK-OV-3 cells and A549/DDP versus A549 cells, but GSTM was induced only in SK-OV-3/DDP cells⁷ (Supplementary Figure S5). Different GST isozymes were thus involved in DDP resistance of different cancer cells, while only GSTA was universally involved, among those cancer cells tested⁷. The treatment with DDP plus siRNA against GSTA, GSTP and GSTM increased apoptosis in A549/DDP versus A549 cells⁷ and SGC7901/DDP versus SGC7901 cells⁷, but the treatment with DDP plus siRNA against GSTA or GSTM rather than GSTP increased apoptosis in

COC1/DDP (Supplementary Note S2-A6 and Figures S6 and S7) and SK-OV-3/DDP cells⁷. Fortunately, the divalent conjugate of BDEA or EDEA showed reasonable inhibition potency against GSTA (Supplementary Table S1). Therefore, BDEA or EDEA at relatively low levels may sensitise DDP-resistant ovarian cancer cells, while BDEA or EDEA at reasonably high concentrations may sensitise all of the tested DDP-resistant cancer cells.

Sensitisation to DDP of DDP-resistant cancers in vitro by the divalent pro-inhibitors

By CCK-8 assay, the IC_{50} value of DDP was \sim 4-fold in SK-OV-3/DDP cells versus SK-OV-3 cells, \sim 7-fold in A549/DDP cells versus A549 cells, \sim 4-fold in COC1/DDP cells versus COC1 cells, and \sim 3-fold in SGC7901/DDP cells versus SGC7901 cells (Table 1 and Supplementary Figure S8). The toxicity of EDEA or BDEA alone was tested. EDEA alone at \sim 1.2 μ M showed \sim 10% inhibition of the growth of HEK293, LO2, SGC7901, SGC7901/DDP and SK-OV-3 cells, but \sim 50% inhibition of the growth of COC1/DDP, COC1, A549 and A549/DDP cells (Table 1 and Supplementary Figures S9 and S10). In fact, EDEA alone of just \sim 0.4 μ M and \sim 0.8 μ M were needed for the 10% inhibition on the growth of COC1 and COC1/DDP cells, respectively (Table 1 and Supplementary Figure S9), and \sim 0.7 μ M and \sim 0.5 μ M for A549 and A549/DDP cells, correspondingly (Table 1 and Supplementary Figure S9). Interestingly, EDEA alone at 3.5 μ M still showed just 10% inhibition on the growth of SK-OV-3/DDP, while at 2.5 μ M already caused $>$ 50% inhibition of the growth of SK-OV-3 (Table 1 and Supplementary Figure S9). In contrast, BDEA alone at \sim 0.2 μ M caused 10% inhibition of the growth of LO2, HEK293, COC1 and COC1/DDP cells, while \sim 1.0 μ M and 4.8 μ M were needed for the \sim 10% inhibition of the growth of SK-OV-3 and SK-OV-3/DDP cells, respectively (Table 1 and Supplementary Figure S10). Notably, BDEA alone at \sim 0.7 μ M and 2.5 μ M already caused 50% inhibition of the growth of HEK293 and LO2 cells, respectively (Table 1 and Supplementary Figure S10). Hence, EDEA or BDEA at levels high enough to inhibit the tested GST isozymes (Supplementary Table S1) was still tolerable by the tested cancer cells, and EDEA showed lower cytotoxicity than BDEA to the tested healthy cells.

The tested cancer cells showed comparable tolerance to BDEA or EDEA against the tested healthy cells. The potential

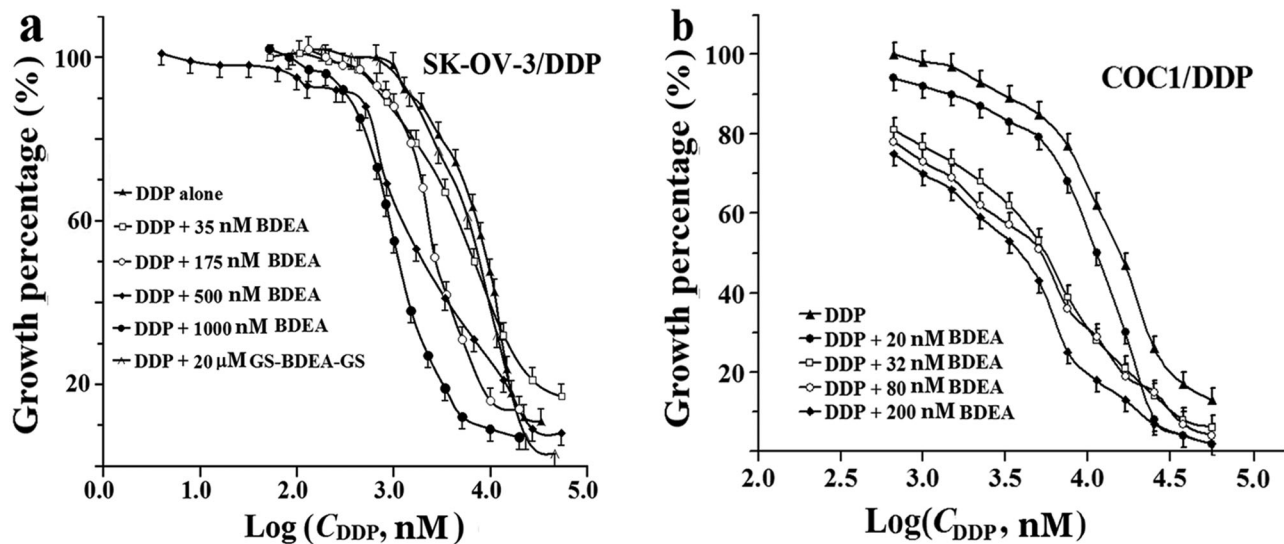


Figure 4. Sensitisation of cancer cells to DDP by BDEA. (a) Sensitisation of SK-OV-3/DDP by BDEA or the divalent conjugate; (b) sensitisation of COC1/DDP by BDEA or the divalent conjugate. The x-axis represented logarithmic molar concentrations of DDP. Cell growth was determined by CCK-8 assay, after cultivation for 72 h since the addition of BDEA or the divalent conjugate, and addition of DDP in 1.0 h later. GS-BDEA-GS: the divalent conjugate of BDEA and GSH. Early and late apoptosis quadrants were being counted. All data were repeated thrice, and expressed in mean \pm SD.

sensitisation actions of BDEA or EDEA were thus examined at the levels tolerated by the healthy cells. BDEA at $0.2 \mu\text{M}$ sensitised SK-OV-3/DDP and COC1/DDP cells to DDP by ~ 3 - and ~ 5 -folds, respectively (Table 1 and Figure 4), but had no significant sensitisation on HEK293, LO2, SK-OV-3, COC1 (Table 1 and Figures S11–14). There were concentration-dependent synergistic actions of BDEA with DDP in SK-OV-3/DDP and COC1/DDP cells, and BDEA at $\sim 40 \text{ nM}$ was still effective to both DDP-resistant cancer cells (Table 1 and Figure 4(a)). BDEA at $\sim 40 \text{ nM}$ should inhibit only GSTM and exhibit negligible cytotoxicity. BDEA may be a sensitizer of the tested resistant ovarian cancers to DDP and a promising tool to probe the roles of GSTM in cellular activities. Unfortunately, the purified divalent conjugate of BDEA and GSH at $20.0 \mu\text{M}$ showed no sensitisation action on SK-OV-3/DDP cells (Figure 4(a)), supporting the crucial roles of membrane permeability in the sensitisation actions of GST isozyme-selective inhibitors. EDEA at $0.5 \mu\text{M}$ showed negligible sensitisation to DDP on all of the tested healthy cells and cancer cells (Table 1 and Supplementary Figures S15, S16, S17a and S18a). Fortunately, EDEA at $1.0 \mu\text{M}$ showed ~ 5 -fold sensitisation on SK-OV-3/DDP cells but negligible sensitisation on SK-OV-3 cells (Table 1 and Supplementary Figure S17), ~ 7 -fold sensitisation to DDP on both A549/DDP and A549 cells (Table 1 and Supplementary Figure S18), and also ~ 2 -fold sensitisation to DDP on both COC1 and COC1/DDP cells (Table 1 and Supplementary Figure S19). However, after the correction of the toxicity action of EDEA alone, there were no sensitisation actions of COC1/DDP and COC1 to DDP by EDEA (Table 1). EDEA showed just detectable synergistic actions at $1.0 \mu\text{M}$, but nearly 5-fold synergistic actions at $1.5 \mu\text{M}$, with DDP on SGC7901/DDP cells (Table 1 and Supplementary Figure S20). EDEA thus exhibited weaker sensitisation actions than BDEA on tested DDP-resistant cancer cells.

The actions of DDP putatively involved the induction of apoptosis of cancer cells¹. The synergetic effect of the designed pro-inhibitors with DDP on the apoptosis of DDP-resistant cancer cells was thus examined. The treatments with DDP alone at $2.0 \mu\text{M}$ in all tested DDP-resistant cancer cells, BDEA alone at up to $1.0 \mu\text{M}$ in SK-OV-3/DDP and at $0.2 \mu\text{M}$ in COC1/DDP cells (Figure 5), and EDEA alone at $1.0 \mu\text{M}$ and $2.0 \mu\text{M}$ in SK-OV-3/DDP, A549/DDP and

SGC7901/DDP cells (Supplementary Figures S21–S23), did not greatly alter the apoptosis percentages. However, the co-treatment with $2.0 \mu\text{M}$ DDP plus $0.2 \mu\text{M}$ BDEA resulted in a ~ 3 -fold increase in apoptosis percentages of SK-OV-3/DDP cells (Figure 5(a)), and ~ 5 -fold increase in apoptosis percentages of COC1/DDP cells (Figure 5(b)), after the correction of the actions of EDEA alone. The co-treatment caused an over ~ 2 -fold increase in apoptosis percentages in SK-OV-3/DDP with $1.5 \mu\text{M}$ DDP plus $2.0 \mu\text{M}$ EDEA (Supplementary Figure S21), and ~ 4 -fold increase in apoptosis percentages in both A549/DDP and SGC7901/DDP cells with $2 \mu\text{M}$ DDP plus $2.0 \mu\text{M}$ EDEA (Supplementary Figures S22 and S23), after the correction of the actions of EDEA alone.

After the treatment of SK-OV-3/DDP cells with $0.2 \mu\text{M}$ BDEA plus $1.5 \mu\text{M}$ DDP, DAPI staining and electron microscopy showed typical changes of apoptotic cells (Supplementary Figure S24), and the release of cytochrome c from mitochondria (Figure 6), while Western blotting indicated the upregulation of caspase 3 and down-regulation of Bcl-2 (Supplementary Figure S25). Therefore, the promotion of cell apoptosis was involved in the synergistic actions of EDEA or BDEA plus DDP on the tested DDP-resistant cancers *in vitro*.

Sensitisation by EDEA to DDP-resistant cancer xenograft models *in vivo*

The lower cytotoxicity of EDEA and reasonable suspension stability of EDEA formulation supported the test of its potential sensitisation actions *in vivo*. For the preliminary test of the pharmacological action of EDEA *in vivo*, a solution of EDEA in DMSO was diluted with 0.2% Tween 80 in physiological saline to a final DMSO concentration of 0.1%. The dose of EDEA administered to nude mice *via* groyne injection was limited by tolerable quantities of DMSO and the aqueous solution. After groyne injection of 0.30 ml of 0.1% DMSO, EDEA at the dose of $1.7 \mu\text{g/g}$ body weight of the nude mice caused no significant toxicity over two weeks, according to the physical morphology, appetite, emotion, and body weights of the tested mice, and further pathological examinations of their livers and kidneys (Supplementary Figure S26). However, differences in the volumes and weights of SK-OV-3/DDP

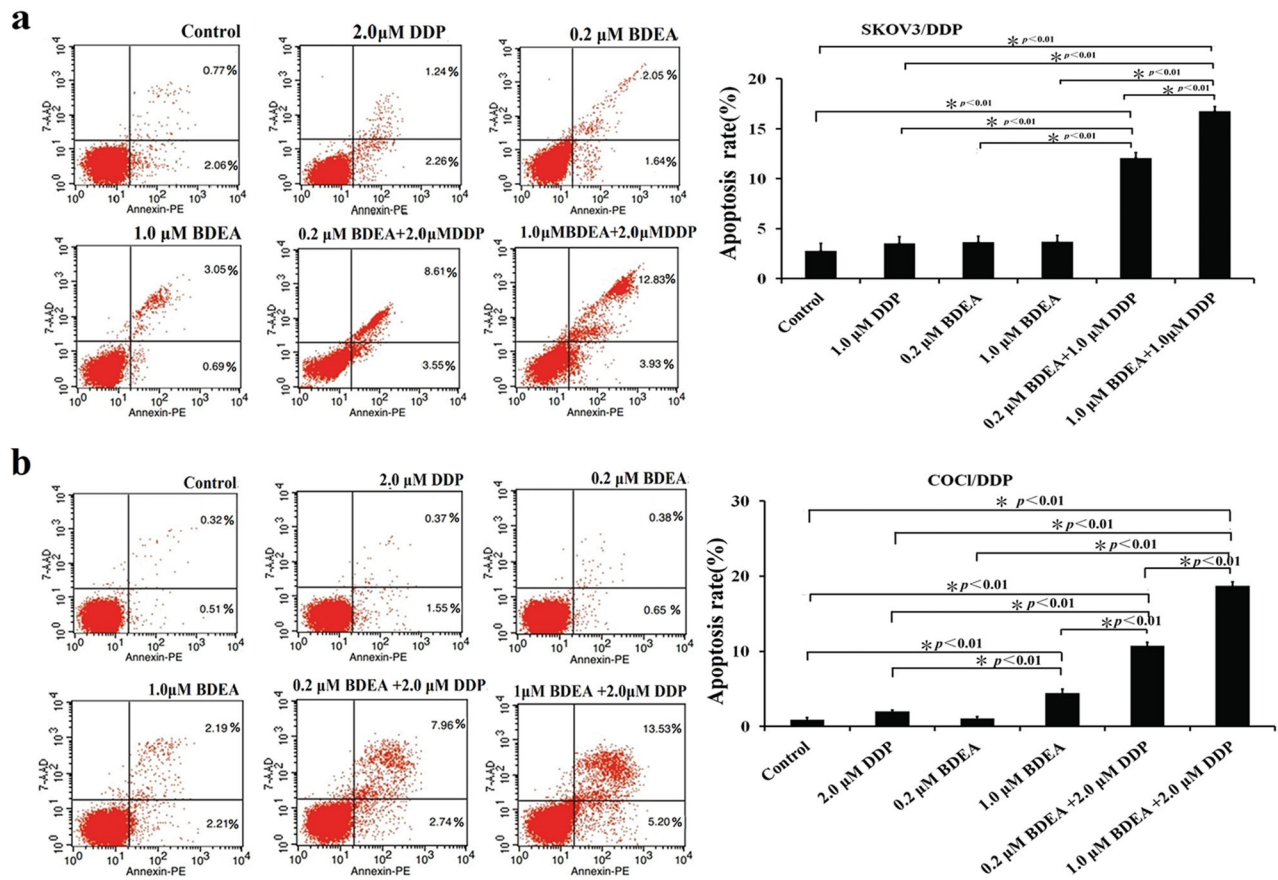


Figure 5. Effects of BDEA plus DDP on apoptosis of the test cells. (a) Effect of BDEA plus DDP on SK-OV-3/DDP. (b) Effect of BDEA plus DDP on COCI/DDP. Early apoptosis and late apoptosis quadrants were being counted for apoptosis rates. All data were repeated thrice, and expressed in mean ± SD. One-way ANOVA followed by a Newman-Keuls *post hoc* test was used for comparison. * $p < 0.05$.

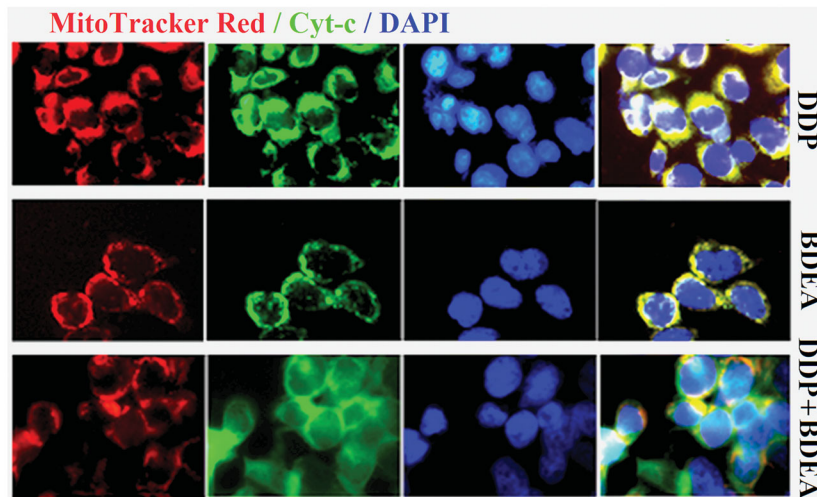


Figure 6. Release of cytochrome c from mitochondria in SK-OV-3/DDP after the treatment with BDEA and DDP. Three treatments utilised the conditions of 1.0 μM DDP, 0.2 μM BDEA and 0.2 μM BDEA + 1.0 μM DDP.

xenograft tumours supported the strong sensitisation actions to DDP *in vivo* by EDEA ($p = 0.01$) (Figure 7). Histological staining of SK-OV-3/DDP xenograft tumours supported the increased apoptosis of cells *in vivo* (Supplementary Figure S27). Unfortunately, EDEA at the same dose showed insignificant sensitisation to DDP in A549/DDP and SGC7901/DDP xenograft models *in vivo*. EDEA thus sensitised SK-OV-3/DDP in the xenograft model, potentially *via* the promotion of cell apoptosis.

Discussion

The actions of GST inhibitors on cells require membrane permeability of the inhibitors and thus lead to the design of pro-inhibitors of GST, which exhibit reasonable membrane permeability and whose products are expected to be potent isozyme-selective inhibitors. The structural differences among tested GST isozymes supported the design of short divalent GSH conjugates as GSTM-selective inhibitors^{24–27}. The divalent GSH conjugates of BDEA and

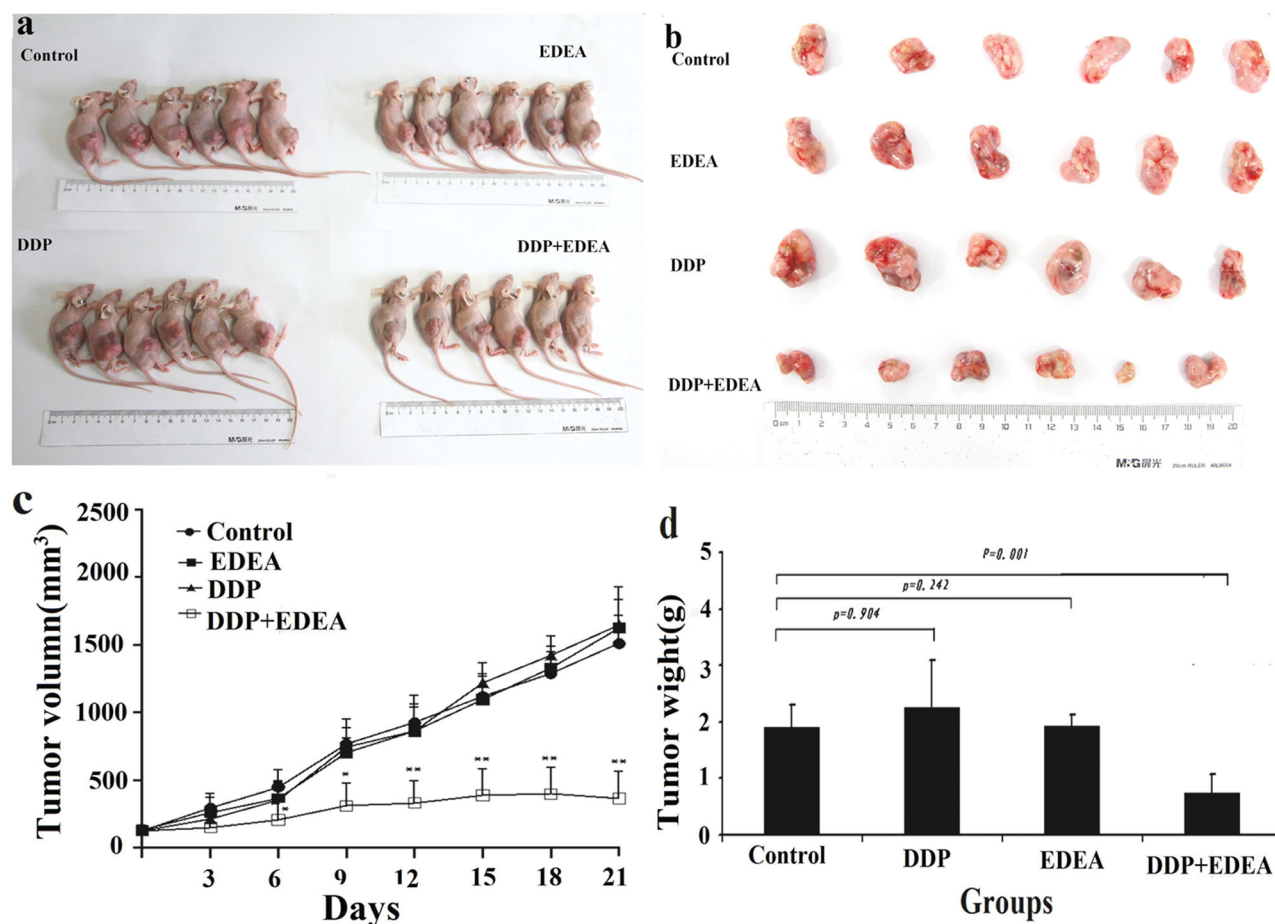


Figure 7. Sensitisation of the xenograft model of SK-OV-3/DDP in nude mice. EDEA at 1.7 mg/kg to DDP at 3.3 mg/kg after continued treatment (once every 3 days). (a) Nude mouse executed three weeks later; (b) photographic views of exercised tumours; (c) comparison of volumes of tumours; (d) comparison of weights of exercised tumours. The photographic images were obtained with CANON DIGITAL 1XUS860IS. All data were repeated thrice, and expressed in mean \pm SD. One-way ANOVA followed by a Newman-Keuls *post hoc* test was used for comparison. * $p < 0.05$.

EDEA were slow tight-binding inhibitors to GSTM but conventional inhibitors to GSTA and GSTP (Supplementary Table S1), and showed the highest affinities to GSTM among the data searchable to date. Among the tested DDP-resistant cancers, SK-OV-3/DDP showed the highest total activity of GSTs and the largest percentage of GSTM activity (Figure 3), and the expected susceptibility to the sensitisation action of BDEA and EDEA at relatively low levels *in vitro*. COC1/DDP is unsuitable for developing a xenograft model *in vivo* but was sensitised to DDP by BDEA and EDEA *in vitro* (Figure 4). EDEA at a dose causing no manifest acute toxicity sensitised to DDP of the SK-OV-3/DDP xenograft model *in vivo* (Figure 7). The small increases in the percent of GSTM activity to total GST activity (Figure 3) versus the susceptible parental cells may account for the insignificant sensitisation to DDP by EDEA in A549/DDP and SGC7901/DDP *in vivo*. EAA at $\sim 20 \mu\text{M}$ also sensitised drug-resistant cancers to DDP *in vitro* but caused manifest toxicity⁹. EDEA and BDEA at levels tolerable by healthy cells still sensitised the tested DDP-resistant cancer cells *in vitro*. The divalent GSH conjugate of BDEA showed undetectable sensitisation on the tested cancer cells due to its negligible membrane permeability. Therefore, BDEA and EDEA were promising leads as both probes to the biological and pharmacological roles of GSTM in cellular activities and sensitisers to DDP in tested DDP-resistant ovarian cancer cells.

The molecular details for the sensitisation of the tested DDP-resistant cancers to DDP by BDEA and EDEA are still puzzling. Three mechanisms have been suggested for the roles of GSTs in

DDP resistance of cancer cells, including GST-catalysed conjugation of both intracellular DDP and its secondary mediators to GSH and/or direct sequestering of DDP by complexing with GSTs, the enhancement of DDP efflux by cell membrane transporters like multidrug resistance-associated protein 2 (MRP2) through the synergistic actions of GSTs by an unsolved molecular mechanism^{1,2,6,10-12}, and the direct binding of GSTs as modulators to signalling proteins that promote cell apoptosis due to the actions of the secondary mediators generated inside cells under the actions of DDP^{8,13-16}. Unfortunately, those three tested GST isozymes did not effectively catalyse GSH conjugation of DDP and were not inhibited by DDP or its conjugate with GSH (data not given). GSTP and GSTM at micromolar levels were found to directly sequester DDP by complexing with DDP through two solvent-accessible reactive residues on their dimers to reduce DDP availability^{31,45}. However, the total molar quantities of GSTP and GSTM in cells are quite small and thus surely limited the contribution of such a direct sequestering pathway to the resistance of cancer cells to DDP. Moreover, the enhancement of DDP efflux by its membrane transporters (especially MRP2) through the synergistic actions of GSTs is widely reported but the molecular mechanisms of such a pathway remains a puzzle^{1,2,6,10-12}. On the other hand, only when the interactions of GSTM with apoptosis signalling proteins are susceptible to the binding of the divalent GSH conjugate of BDEA or EDEA to GSTM, the third pathways can play some roles in both the DDP resistance of the tested DDP-resistant cancer cells and their sensitisation to DDP by BDEA and EDEA, but

its verification remains a challenge. Fortunately, some intracellular secondary mediators of DDP actions promote the apoptosis of cancer cells^{1,2,6,10,46–48}; the treatment with DDP plus EDEA increased apoptosis of the tested DDP-resistant cancer cells *in vitro* and the SK-OV-3/DDP xenograft model *in vivo* (Figure 7). EDEA or BDEA may thus inhibit GST activity to restore the intracellular levels of those secondary mediators that promote cancer cell apoptosis; such an indirect pathway of GSTM action can at least partially account for the sensitisation of the tested resistant cancer cells to DDP by EDEA and BDEA. Unfortunately, such intracellular secondary mediators under the actions of DDP have not yet been fully elucidated. Inevitably, more efforts are still mandatory to elucidate the molecular mechanisms of DDP resistance in the tested DDP-resistant cancer cells and their sensitisation to DDP by BDEA and EDEA.

In conclusion, based on the accessibility to the cleft linking two active sites and the distance between the G-sites of the two active sites of GST dimers, divalent pro-inhibitors BDEA and EDEA with short linear diamines to link ethacrynic acid were designed against GSTM; their divalent GSH conjugates were slow tight-binding inhibitors of GSTM but conventional inhibitors of GSTA and GSTP, and concomitantly occupied two active sites of the GSTM dimer. In SK-OV-3/DDP cell lysates, total GST activity and the percent of GSTM activity to total GST activity were considerably large. EDEA showed lower cytotoxicity than BDEA *in vitro*, and sensitised SK-OV-3/DDP to DDP *in vitro* and *in vivo* in a xenograft model of nude mice. BDEA and EDEA designed as divalent pro-inhibitors are thus promising leads of both sensitisers to overcome cancer DDP resistance relying on GSTM actions and tools to reveal biological and pharmacological roles of GSTM in cellular activities. In view of unfavorably large hydrophobicity and thus low solubility as well as potential strong binding to serum albumin of BDEA and EDEA with doubled EA and linear linkers, the balance of membrane permeability and solubility of designed analogues is crucial in the future for further optimisation.

Acknowledgements

The authors are particularly grateful to Professor Deqiang Wang at College of Laboratory Medicine at Chongqing Medical University for his help with the crystallization and diffraction data analysis, Professor Jingyuan Wan at the College of Pharmacy at Chongqing Medical University for his help with the cell experiments; Tinghe Yu at Chongqing Medical University and Qing Wu at Shanghai Jiao Tong University for their donation of the test cells.

Disclosure statement

The authors declare that they have no competing interests.

Funding

This work was supported by National Natural Science Foundation of China (grant nos. 81773625, 81071427, 31570862), Ph.D. Programs Foundation of Ministry of Education of the People's Republic of China (no.20125503110007), Natural Science Foundation Project of Chongqing, Chongqing Science and Technology Commission (CSTC2012JJA0057, CSTC2019jcyj-msxmX0166), Scientific Research Project of the University-Town Hospital of Chongqing Medical University (2021JC03).

ORCID

Xiaolan Yang  <http://orcid.org/0000-0001-9320-1036>
Fei Liao  <http://orcid.org/0000-0001-7671-6871>

References

1. Dasari S, Bernard Tchounwou P. Cisplatin in cancer therapy: molecular mechanisms of action. *Eur J Pharmacol* 2014;740: 364–78.
2. Galluzzi L, Vitale I, Michels J, et al. Systems biology of cisplatin resistance: past, present and future. *Cell Death Dis* 2014;5:e1257.
3. Hanna PE, Anders MW. The mercapturic acid pathway. *Crit Rev Toxicol* 2019;49:819–929.
4. Tew KD, Monks A, Barone L, et al. Glutathione-associated enzymes in the Human Cell Lines of the National Cancer Institute Drug Screening Program. *Mol Pharmacol* 1996;50: 149–59.
5. Morgan AS, Ciaccio PJ, Tew KD, Kauvar LM. Isozyme-specific glutathione S-transferase inhibitors potentiate drug sensitivity in cultured human tumor cell lines. *Cancer Chemother Pharmacol* 1996;37:363–70.
6. Pljesa-Ercegovac M, Savic-Radojevic A, Matic M, et al. Glutathione transferases: potential targets to overcome chemoresistance in solid tumors. *Int J Mol Sci* 2018;19: 3785–805.
7. Zou M, Hu X, Xu B, et al. Glutathione S-transferase isozyme alpha 1 is predominantly involved in the cisplatin resistance of common types of solid cancer. *Oncol Rep* 2019;41: 989–98.
8. Singh RR, Reindl KM. Glutathione S-transferases in cancer. *Antioxidants (Basel)* 2021;10:701–25.
9. Schultz M, Dutta S, Tew KD. Inhibitors of glutathione S-transferases as therapeutic agents. *Adv Drug Deliv Rev* 1997; 26:91–104.
10. Sau A, Pellizzari Tregno F, Valentino F, et al. Glutathione transferases and development of new principles to overcome drug resistance. *Arch Biochem Biophys* 2010;500: 116–22.
11. Smitherman PK, Townsend AJ, Kute TE, Morrow CS. Role of multidrug resistance protein 2 (MRP2, ABC2) in alkylating agent detoxification: MRP2 potentiates glutathione S-transferase A1-1-mediated resistance to chlorambucil cytotoxicity. *J Pharmacol Exp Ther* 2004;308:260–7.
12. Depeille P, Cuq P, Mary S, et al. Glutathione S-transferase M1 and multidrug resistance protein 1 act in synergy to protect melanoma cells from vincristine effects. *Mol Pharmacol* 2004;65:897–905.
13. Lo HW, Ali-Osman F. Genetic polymorphism and function of glutathione S-transferases in tumor drug resistance. *Curr Opin Pharmacol* 2007;7:367–74.
14. Cho SG, Lee YH, Park HS, et al. Glutathione S-transferase mu modulates the stress-activated signals by suppressing apoptosis signal-regulating kinase 1. *J Biol Chem* 2001;276: 12749–55.
15. Chatterjee A, Gupta S. The multifaceted role of glutathione S-transferases in cancer. *Cancer Lett* 2018;433:33–42.
16. Laborde E. Glutathione transferases as mediators of signaling pathways involved in cell proliferation and cell death. *Cell Death Differ* 2010;17:1373–80.

17. Mahajan S, Atkins WM. The chemistry and biology of inhibitors and pro-drugs targeted to glutathione S-transferases. *Cell Mol Life Sci* 2005;62:1221–33.
18. Allocati N, Masulli M, Di Ilio C, Federici L. Glutathione transferases: substrates, inhibitors and pro-drugs in cancer and neurodegenerative diseases. *Oncogenesis* 2018;7:8–22.
19. Stoddard EG, Killinger BJ, Nair RN, et al. Activity-based probes for isoenzyme- and site-specific functional characterization of glutathione S-transferases. *J Am Chem Soc* 2017;139:16032–5.
20. Wang CH, Wu HT, Cheng HM, et al. Inhibition of glutathione S-transferase M1 by new gabosine analogues is essential for overcoming cisplatin resistance in lung cancer cells. *J Med Chem* 2011;54:8574–81.
21. Rotili D, De Luca A, Tarantino D, et al. Synthesis and structure–activity relationship of new cytotoxic agents targeting human glutathione-S-transferases. *Eur J Med Chem* 2015;89:156–71.
22. Federici L, Lo Sterzo C, Pezzola S, et al. Structural basis for the binding of the anticancer compound 6-(7-nitro-2,1,3-benzoxadiazol-4-ylthio)hexanol to human glutathione s-transferases. *Cancer Res* 2009;69:8025–34.
23. Mammen M, Choi S-K, Whitesides GM. Polyvalent interactions in biological systems: implications for design and use of multivalent ligands and inhibitors. *Angew Chem Int Ed* 1998;37:2754–94.
24. Clipson AJ, Bhat VT, McNae I, et al. Bivalent enzyme inhibitors discovered using dynamic covalent chemistry. *Chemistry* 2012;18:10562–70.
25. Mahajan SS, Hou L, Doneanu C, et al. Optimization of bivalent glutathione S-transferase inhibitors by combinatorial linker design. *J Am Chem Soc* 2006;128:8615–25.
26. Maeda DY, Mahajan SS, Atkins WM, Zebala JA. Bivalent inhibitors of glutathione S-transferase: the effect of spacer length on isozyme selectivity. *Bioorg Med Chem Lett* 2006;16:3780–3.
27. Lyon RP, Hill JJ, Atkins WM. Novel class of bivalent glutathione S-transferase inhibitors. *Biochemistry* 2003;42:10418–28.
28. Koehler RT, Villar HO, Bauer KE, Higgins DL. Ligand-based protein alignment and isozyme specificity of glutathione S-transferase inhibitors. *Proteins: Struct Funct Genet* 1997;28:202–16.
29. Ata A, Udenigwe CC. The discovery and application of inhibitors of glutathione S-transferase as therapeutic agents – a review. *Curr Bioact Compd* 2008;4:41–50.
30. Ploemen JHTM, Ommen BV, Bogaards JJP, Bladeren PJV. Ethacrynic acid and its glutathione conjugate as inhibitors of glutathione S-transferases. *Xenobiotica* 1993;23:913–23.
31. Parker LJ, Italiano LC, Morton CJ, et al. Studies of glutathione transferase P1-1 bound to a platinum(IV)-based anticancer compound reveal the molecular basis of its activation. *Chemistry* 2011;17:7806–16.
32. Lipinski CA, Lombardo F, Dominy BW, Feeney PJ. Experimental and computational approaches to estimate solubility and permeability in drug discovery and development settings. *Adv Drug Deliv Rev* 1997;23:3–25.
33. Lo W-J, Chiou Y-C, Hsu Y-T, et al. Enzymatic and nonenzymatic synthesis of glutathione conjugates: application to the understanding of a parasite's defense system and alternative to the discovery of potent glutathione S-transferase inhibitors. *Bioconjug Chem* 2007;18:109–20.
34. McIlwain CC, Townsend DM, Tew KD. Glutathione S-transferase polymorphisms: cancer incidence and therapy. *Oncogene* 2006;25:1639–48.
35. Yang X, Du Z, Pu J, et al. Classification of difference between inhibition constants of an inhibitor to facilitate identifying the inhibition type. *J Enzyme Inhib Med Chem* 2013;28:205–13.
36. Xu B, Tan D, Yang X, et al. Fluorometric titration assay of affinity of tight-binding nonfluorescent inhibitor of glutathione S-transferase. *J Fluoresc* 2015;25:1–8.
37. Williams JW, Morrison JF. The kinetics of reversible tight-binding inhibition. *Methods Enzymol* 1979;63:437–67.
38. Caffrey PB, Frenkel GD, McAndrew KL, Marks K. A model of the development of cisplatin resistance in human small cell lung cancer xenografts. *In Vivo* 2016;30:745–9.
39. Chen B, Ke L, Xia G, et al. Reversal of multidrug resistance by cisplatin-loaded magnetic Fe₃O₄ nanoparticles in A549/DDP lung cancer cells in vitro and in vivo. *Int J Nanomedicine* 2013;8:1867–77.
40. Rossmann MG, Beek CGv. Data processing. *Acta Crystallogr D Biol Crystallogr* 1999;55:1631–41.
41. McCoy AJ, Grosse-Kunstleve RW, Adams PD, et al. Phaser crystallographic software. *J Appl Crystallogr* 2007;40:658–74.
42. Emsley P, Cowtan K. Coot: model-building tools for molecular graphics. *Acta Crystallogr D Biol Crystallogr* 2004;60:2126–32.
43. Adams PD, Afonine PV, Bunkoczi G, Chen VB, et al. PHENIX: a comprehensive Python-based system for macromolecular structure solution. *Acta Crystallogr D Biol Crystallogr* 2010;66:213–21.
44. Buist HE, van Burgsteden JA, Freidig AP, et al. New in vitro dermal absorption database and the prediction of dermal absorption under finite conditions for risk assessment purposes. *Regul Toxicol Pharmacol* 2010;57:200–9.
45. De Luca A, Parker LJ, Ang WH, et al. A structure-based mechanism of cisplatin resistance mediated by glutathione transferase P1-1. *Proc Natl Acad Sci U S A* 2019;116:13943–51.
46. Yan X-D, Pan L-Y, Yuan Y, et al. Identification of platinum-resistance associated proteins through proteomic analysis of human ovarian cancer cells and their platinum-resistant sub-lines. *J Proteome Res* 2007;6:772–80.
47. Piaggi S, Raggi C, Corti A, et al. Glutathione transferase omega 1-1 (GSTO1-1) plays an anti-apoptotic role in cell resistance to cisplatin toxicity. *Carcinogenesis* 2010;31:804–11.
48. Pathania S, Bhatia R, Baldi A, et al. Drug metabolizing enzymes and their inhibitors' role in cancer resistance. *Biomed Pharmacother* 2018;105:53–65.